

GLASMA FLUCTUATIONS AT FINITE
PROPER TIMES*

PABLO GUERRERO-RODRÍGUEZ

LIP, Av. Prof. Gama Pinto, 2, 1649-003 Lisbon, Portugal

*Received 29 November 2022, accepted 13 January 2023,**published online 25 May 2023*

By describing the initial stage of heavy-ion collisions in terms of freely-evolving classical fields, we calculate the energy density of one- and two-point correlation functions at finite proper times. With this approach, we are able to effectively resum the high-momentum terms of a power series expansion in proper time, thus making it convergent. Our results provide analytical insight into the dynamics of the Glasma phase.

DOI:10.5506/APhysPolBSupp.16.5-A19

The Glasma is a highly dense, out-of-equilibrium substance that emerges right after heavy-ion collisions (HICs). This initial state quickly evolves through multiple scatterings of its components, and eventually thermalizes into a quark–gluon plasma (QGP). The QGP expands and cools down in a process that can be described with viscous hydrodynamics, and eventually, its components rearrange into individual hadrons. The resulting hadron gas finally flies off through the detectors, along with other kinds of radiation. Through the analysis of these final-state particles, it is possible to extract information about the properties of the QGP. However, the interpretation of these studies is often hindered by several uncertainties, both on the theoretical and experimental sides. In this work, we focus on a specific source of uncertainty: the description of initial-stage fluctuations. Specifically, we consider those that arise from the quantum fluctuations of the wave functions of the colliding nuclei. A convenient aspect of this particular effect is that, in principle, we should be able to describe it with quantum chromodynamics (QCD), without relying (too much) on phenomenological models. In order to characterize the effect of quantum fluctuations over specific properties of the medium, we compute the following objects: $\langle \varepsilon(x_\perp) \rangle$, $\langle \dot{\nu}(x_\perp) \rangle$, $\langle \varepsilon(x_\perp) \varepsilon(y_\perp) \rangle$, $\langle \dot{\nu}(x_\perp) \dot{\nu}(y_\perp) \rangle$. These are the one- and two-point correlators of the distributions of energy density ε and the divergence of the Chern–Simons current $\dot{\nu}$

* Presented at the Diffraction and Low- x 2022 Workshop, Corigliano Calabro, Italy, 24–30 September, 2022.

(which controls the generation of axial charge) deposited in the transverse plane to the collision axis. We perform these calculations in a high-energy approximation of QCD called color glass condensate (CGC), where we treat the large densities of soft (small- x) gluons carried by the colliding nuclei as classical fields emitted by the valence quarks. The dynamics of these fields follow from the Yang–Mills equations, $[D_\mu, F^{\mu\nu}] = J^\nu \propto \rho(x_\perp)$. Here, the sources of the fields would be the static color currents J^μ , which represent the valence quarks of the nuclei. In order to account for the fluctuations, we treat the transverse distributions of color charges ρ as random variables that obey Gaussian statistics (McLerran–Venugopalan [MV] model). The correlators of observables are then obtained as functional averages over all possible color charge configurations. In this framework, it is possible to compute our correlators analytically in a very restricted region of space-time, namely: an infinitesimal proper time after the collision, $\tau = 0^+$. These calculations have been performed previously in several works [1–4], and they play the role of initial conditions for the subsequent proper time evolution of the system. This evolution is encoded in the Yang–Mills equations with two sources, which unfortunately do not have an analytical solution. Apart from numerical methods, other approaches to this problem have relied on analytical approximations such as the weak field limit [1, 5, 6] or the expansion in powers of proper time [7–9]. However, these strategies come with significant downsides and restrictions, namely: the weak field limit is only applicable in the dilute-dense regime, and the proper time expansion carries numerous UV divergences on each term. In this work, we propose that the fact that we want to compute largely UV-dominated quantities allows us to describe their evolution with a linearized version of the Yang–Mills equations

$$\partial_\tau \frac{1}{\tau} \partial_\tau (\tau^2 \beta) = \tau \partial_i \partial^i \beta, \quad (1)$$

$$\partial_\tau (\tau \partial_\tau \beta^i) = \tau \partial^k \partial_k \beta^i. \quad (2)$$

Of course, for this approximation to be reasonable one needs to work in an appropriate gauge: one that minimizes the neglected terms. A natural choice is given by the Coulomb gauge ($\partial_i \beta^i = 0$), which minimizes the amplitudes of the transverse components of the fields. By assuming (1) that this condition is satisfied, (2) a free dispersion relation ($\omega(k_\perp) = |k_\perp| \equiv k$), and (3) that the fields match the results obtained at $\tau = 0^+$, one finds the following solution:

$$\beta(\tau, k_\perp) = \frac{\tau}{k} E_0^\eta(k_\perp) J_1(k\tau), \quad (3)$$

$$\beta^i(\tau, k_\perp) = -i \frac{\epsilon^{ij} k^j}{k^2} B_0^\eta(k_\perp) J_0(k\tau), \quad (4)$$

which effectively resums the aforementioned UV singularities (making the corresponding power series finite). These expressions can be essentially described as the free-wave propagation of the initial conditions (E_0^η and B_0^η). This is a reasonable approximation for high momentum modes which, conveniently, are the most dominant contributions for both ε and $\dot{\nu}$. Another crucial assumption that is implicit in this calculation is that we have transformed our initial conditions to the Coulomb gauge. This is something that can be done analytically only in the dilute-dense case. Here, what we do instead is using a gauge field that for finite values of τ satisfies linear Yang–Mills evolution in the Coulomb gauge, and, at $\tau = 0^+$, reproduces the initial conditions for the electric and magnetic fields. Note that this is not necessarily true for the gauge fields themselves; we impose this condition for the electric and magnetic fields only. In so doing, we are basically taking advantage of the fact that the objects that we want to study can be expressed purely in terms of the electric and magnetic fields (not explicitly in terms of the gauge fields).

Having obtained the τ -dependent gauge fields as a function of the initial conditions, the ensuing calculation of one-point correlators requires knowledge of the two-point function of the $\tau = 0^+$ Glasma fields $\langle \alpha_u^{i,a}(u_\perp) \alpha_v^{k,c}(v_\perp) \rangle \equiv \langle \alpha_u^{i,a} \alpha_v^{k,c} \rangle$. By adopting the Golec-Biernat–Wusthoff (GBW) model, we obtain that $\langle \dot{\nu} \rangle = 0$ (for any value of τ) and

$$\begin{aligned} \langle \varepsilon(\tau, x_\perp) \rangle &= \frac{g^2}{2} \left(\delta^{ij} \delta^{kl} + \epsilon^{ij} \epsilon^{kl} \right) f^{abn} f^{cdn} \int_{u,v} \langle \alpha_u^{i,a} \alpha_v^{k,c} \rangle_1 \langle \alpha_u^{j,b} \alpha_v^{l,d} \rangle_2 \\ &\quad \times \frac{\delta(|x_\perp - u_\perp| - \tau)}{2\pi\tau} \frac{\delta(|x_\perp - v_\perp| - \tau)}{2\pi\tau} (1 + \cos(\theta_{x-u} - \theta_{x-v})). \end{aligned} \quad (5)$$

This is a particularly transparent expression: the average energy density results from the interference of the Weizsäcker–Williams distributions characterizing each nucleus, with a trigonometric factor controlling whether the interference is constructive or destructive. At this point, if we substitute the two-point function from the GBW model and solve (most of) the resulting integrals, we eventually arrive at

$$\begin{aligned} \langle \varepsilon(\tau, x_\perp) \rangle &= \frac{g^2}{2} N_c (N_c^2 - 1) \int \frac{d\Theta}{2\pi} (1 + \cos(\Theta)) \\ &\quad \times \left(\frac{Q_{s1}^2}{g^2 N_c} \frac{1 - \exp\left\{-\frac{Q_{s1}^2 \tau^2}{2}(1 - \cos(\Theta))\right\}}{\frac{Q_{s1}^2 \tau^2}{2}(1 - \cos(\Theta))} \right) \times (1 \rightarrow 2) \\ &\equiv \langle \varepsilon_0 \rangle \times \phi(Q_{s1}\tau, Q_{s2}\tau), \end{aligned} \quad (6)$$

where $\Theta = \theta_{x-u} - \theta_{x-v}$. The remaining integral is calculated numerically. In the last line, we remark that the effect of τ -evolution can be described

as the initial energy density $\langle \varepsilon_0 \rangle$ times a non-trivial dilution factor ϕ , which describes the decrease of the average energy density with time (in units of the saturation scales of each nucleus). In Fig. 1 (left) we display ϕ as a function of $Q_s \tau$ for both GBW and MV models. This plot shows that the average energy density decrease is remarkably more pronounced for the MV model than for the GBW model, especially at early proper times.

By repeating the previous steps in the case of the two-point functions, we eventually arrive at

$$\begin{aligned}
\langle \varepsilon(\tau, x_\perp) \varepsilon(\tau, y_\perp) \rangle &= \frac{g^4}{8} N_c^2 (N_c^2 - 1) \int_0^{2\pi} \frac{d\theta_s}{2\pi} \frac{d\theta_{\bar{s}}}{2\pi} \frac{d\theta_t}{2\pi} \frac{d\theta_{\bar{t}}}{2\pi} \\
&\times (1 + \cos(\theta_s - \theta_{\bar{s}}))(1 + \cos(\theta_t - \theta_{\bar{t}})) \\
&\times \left[\left((N_c^2 - 1) G_1((s - \bar{s})_\tau) G_1((t - \bar{t})_\tau) G_2((s - \bar{s})_\tau) G_2((t - \bar{t})_\tau) \right. \right. \\
&+ 2G_1((s - \bar{s})_\tau) G_1((t - \bar{t})_\tau) G_2((s - t)_\tau - r_\perp) G_2((\bar{s} - \bar{t})_\tau - r_\perp) \\
&+ G_1((s - t)_\tau - r_\perp) G_1((\bar{s} - \bar{t})_\tau - r_\perp) G_2((s - t)_\tau - r_\perp) G_2((\bar{s} - \bar{t})_\tau - r_\perp) \left. \right) \\
&+ \left(1 \leftrightarrow 2 \right) \Big], \tag{7}
\end{aligned}$$

$$\begin{aligned}
\langle \dot{\nu}(\tau, x_\perp) \dot{\nu}(\tau, y_\perp) \rangle &= \frac{g^4}{64} N_c^2 (N_c^2 - 1) \int_0^{2\pi} \frac{d\theta_s}{2\pi} \frac{d\theta_{\bar{s}}}{2\pi} \frac{d\theta_t}{2\pi} \frac{d\theta_{\bar{t}}}{2\pi} \\
&\times (1 + \cos(\theta_s - \theta_{\bar{s}}))(1 + \cos(\theta_t - \theta_{\bar{t}})) \\
&\times \left[\left(G_1((s - t)_\tau - r_\perp) G_1((\bar{s} - \bar{t})_\tau - r_\perp) G_2((s - \bar{t})_\tau - r_\perp) G_2((\bar{s} - t)_\tau - r_\perp) \right. \right. \\
&+ 2G_1((s - t)_\tau - r_\perp) G_1((\bar{s} - \bar{t})_\tau - r_\perp) G_2((s - t)_\tau - r_\perp) G_2((\bar{s} - \bar{t})_\tau - r_\perp) \left. \right) \\
&+ \left(1 \leftrightarrow 2 \right) \Big], \tag{8}
\end{aligned}$$

where we used the GBW model and assumed that the four-point function of gluon field decomposes into products of two-point functions (*i.e.* Glasma graph approximation). The remaining integration over four angular variables is performed numerically for every value of τ and correlation distance $r = |x_\perp - y_\perp|$. In so doing, we obtain the curves shown in Fig. 1 (right) (see [10] to find curves corresponding to the MV model).

On a quick look at Fig. 1 (right), one could describe the general trend of the evolution as an increase in the correlation length, which is one of the effects expected to take place in any system that is approaching the

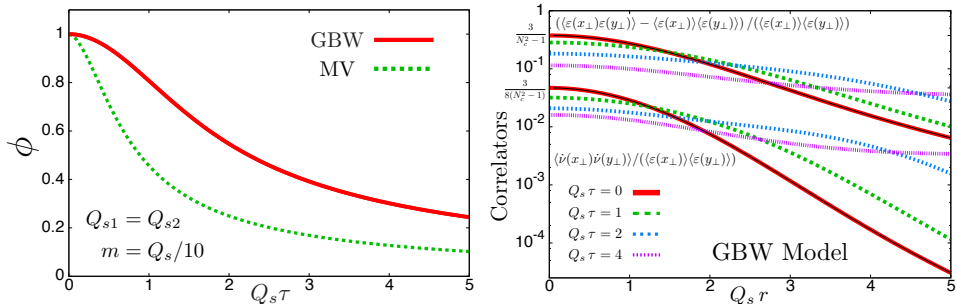


Fig. 1. Left: Dilution function for the GBW and MV models (considering identical nuclei). Right: Correlation functions of the energy density and the divergence of the Chern–Simons current at different values of τ for the GBW model.

hydrodynamical regime. This is in agreement with our intuition of how the τ -evolution should act upon our correlators. This is not, however, the whole story, as we do not expect our fundamental assumptions to be valid throughout the whole pre-equilibrium period. Indeed, the calculations discussed above are based on a classical approximation that will eventually break down as the system expands and becomes dilute. At that point, it has been argued that an effective kinetic theory would provide the intermediate step that matches the classical description with hydrodynamics (*e.g.* [11]).

Upon further refining of our calculations (*e.g.* going beyond the Glasma graph approximation), our results could be applied to constrain the initial conditions of hydrodynamical evolution, describe eccentricity fluctuations, as well as potentially save computing time for models based on numerical solutions to the Yang–Mills equations.

Despite its limitations, the classical approximation can still provide many interesting results regarding the study of initial-stage fluctuations. For instance, in the case of proton–nucleus collisions, one may expand the previous calculation by adding hot-spot fluctuations on top of the CGC fluctuations discussed above. Within this framework, the correlators are computed differently depending on the nucleus. On the one hand, the averages over color source densities of the dense nucleus, ρ_1 , are the typical CGC averages. However, in the case of the color source densities corresponding to the dilute nucleus, ρ_2 , these correlators are promoted to double correlators

$$\langle\langle \mathcal{O}(\rho_2) \rangle\rangle = \left(\frac{2\pi R^2}{N_q} \right) \int \prod_{i=1}^{N_q} [d^2 \mathbf{b}_i T(\mathbf{b}_i - \mathbf{B})] \delta \left(\frac{1}{N_q} \sum_{i=1}^{N_q} \mathbf{b}_i - \mathbf{B} \right) \langle \mathcal{O}(\rho_2) \rangle_{\text{CGC}}. \quad (9)$$

Here, the positions of hot spots fluctuate according to a Gaussian distribution ($T(\mathbf{b}) = \frac{1}{2\pi R^2} \exp\left[-\frac{\mathbf{b}^2}{2R^2}\right]$), and the density of color charges within each hot spot fluctuates too. This framework was applied in [12] to the calculation of energy density correlators at $\tau = 0^+$, as well as eccentricities in proton–nucleus collisions. The generalization of their results to finite values of τ is an ongoing work that will be presented in a future publication.

The author thanks Tuomas Lappi for the collaboration in [10]. The author also wishes to thank Sami Demirci for his ongoing collaboration in the project outlined above. Finally, the author acknowledges financial support from the European research Council projects ERC-2015-CoG-681707 (CGCglasmaQGP) and ERC-2018-ADG-835105 (YoctoLHC).

REFERENCES

- [1] T. Lappi, S. Schlichting, *Phys. Rev. D* **97**, 034034 (2018), [arXiv:1708.08625 \[hep-ph\]](#).
- [2] T. Lappi, *Phys. Lett. B* **643**, 11 (2006), [arXiv:hep-ph/0606207](#).
- [3] J.L. Albacete, P. Guerrero-Rodríguez, C. Marquet, *J. High Energy Phys.* **2019**, 073 (2019), [arXiv:1808.00795 \[hep-ph\]](#).
- [4] P. Guerrero-Rodríguez, *J. High Energy Phys.* **2019**, 026 (2019), [arXiv:1903.11602 \[hep-ph\]](#).
- [5] A. Dumitru, L.D. McLerran, *Nucl. Phys. A* **700**, 492 (2002), [arXiv:hep-ph/0105268](#).
- [6] L. McLerran, V. Skokov, *Nucl. Phys. A* **959**, 83 (2017), [arXiv:1611.09870 \[hep-ph\]](#).
- [7] R.J. Fries, J.I. Kapusta, Y. Li, [arXiv:nucl-th/0604054](#).
- [8] H. Fujii, K. Fukushima, Y. Hidaka, *Phys. Rev. C* **79**, 024909 (2009), [arXiv:0811.0437 \[hep-ph\]](#).
- [9] G. Chen, R.J. Fries, J.I. Kapusta, Y. Li, *Phys. Rev. C* **92**, 064912 (2015), [arXiv:1507.03524 \[nucl-th\]](#).
- [10] P. Guerrero-Rodríguez, T. Lappi, *Phys. Rev. D* **104**, 014011 (2021), [arXiv:2102.09993 \[hep-ph\]](#).
- [11] A. Kurkela *et al.*, *Phys. Rev. C* **99**, 034910 (2019), [arXiv:1805.00961 \[hep-ph\]](#).
- [12] S. Demirci, T. Lappi, S. Schlichting, *Phys. Rev. D* **103**, 094025 (2021), [arXiv:2101.03791 \[hep-ph\]](#).